



# Effects of Provenance, Transport Processes and Chemical Weathering on Heavy Mineral Composition: A Case Study From the Songhua River Drainage, NE China

Peng Wu<sup>1,2</sup>, Yuanyun Xie<sup>1,2\*</sup>, Chunguo Kang<sup>3</sup>, Yunping Chi<sup>1,2</sup>, Lei Sun<sup>1,2</sup> and Zhenyu Wei<sup>1</sup>

<sup>1</sup>College of Geographic Science, Harbin Normal University, Harbin, China, <sup>2</sup>Heilongjiang Province Key Laboratory of Geographical Environment Monitoring and Spatial Information Service in Cold Regions, Harbin Normal University, Harbin, China, <sup>3</sup>College of Geography and Tourism, Harbin University, Harbin, China

## OPEN ACCESS

### Edited by:

Alan R. Butcher,  
Geological Survey of Finland, Finland

### Reviewed by:

Saumitra Kumar Misra,  
University of KwaZulu-Natal, South  
Africa  
Christine Franke,  
Université de Sciences Lettres de  
Paris, France

### \*Correspondence:

Yuanyun Xie  
xyy0451@163.com

### Specialty section:

This article was submitted to  
Sedimentology, Stratigraphy and  
Diagenesis,  
a section of the journal  
Frontiers in Earth Science

**Received:** 20 December 2021

**Accepted:** 05 May 2022

**Published:** 24 May 2022

### Citation:

Wu P, Xie Y, Kang C, Chi Y, Sun L and  
Wei Z (2022) Effects of Provenance,  
Transport Processes and Chemical  
Weathering on Heavy Mineral  
Composition: A Case Study From the  
Songhua River Drainage, NE China.  
Front. Earth Sci. 10:839745.  
doi: 10.3389/feart.2022.839745

Understanding the heavy mineral composition of the Songhua River basin in NE China and the influencing factors (e.g., provenance, transport processes and chemical weathering) is crucial for the study of both the source-to-sink processes and the drainage evolution in the region. To this end, a total of 43 samples were collected from the river bars and terraces of the main and tributary streams of the Songhua River, and analyzed for heavy minerals in different grain-size fractions based on the novel automated TESCAN Integrated Mineral Analyzer (TIMA) combined with standard optical method. The results show that the tributaries originating from different mountains have significantly different heavy mineral composition. The locally occurring basic source signal in the tributaries of the Nenjiang River (the largest tributary of the Songhua River) are not well preserved in the Nenjiang River and the Songhua River trunk streams, indicating that the control of sources on heavy mineral composition is influenced by fluvial processes. Additionally, significant differences in the heavy mineral composition of different reaches of the same river also indicate that the heavy mineral composition is significantly influenced by fluvial processes. Influenced by hydraulic sorting during river processes, heavy minerals are enriched in different size fractions with the low-density minerals systematically overestimated in a wide window, suggesting an advantage of multi-window policy over wide window policy. In contrast to modern river sediments, the original heavy mineral composition of river terrace sediments has been severely damaged due to chemical weathering, so the degree of chemical weathering of terrace sediments needs to be evaluated first in provenance tracing and paleo-drainage evolution studies. TIMA has an irreplaceable role in identifying mineral species, additional images and elemental composition, and however, it performs poorly in identifying polycrystalline minerals, thus the combination with traditional methods can obtain more complete and accurate information.

**Keywords:** heavy minerals, Songhua River, provenance, fluvial processes, chemical weathering, TIMA analyses

## INTRODUCTION

Heavy mineral analysis, diagnostic of particular sources, is a powerful technique in constraining sediment provenance, tectonic history (Mange and Wright, 2007; Vezzoli et al., 2016; Zhang et al., 2020), and thus deciphering the lithological and mineralogical information of the rocks exposed in the source area (Morton and Hallsworth, 1999; Morton et al., 2005; Morton and Hallsworth, 2007; Krippner et al., 2015; Zhang et al., 2015). However, heavy mineral assemblages in fluvial sediments may be modified by many factors during the generation-transport-deposition and post-sedimentary processes (e.g., lithology, hydrodynamic sorting, weathering, mechanical breakdown and diagenesis; Krippner et al., 2016; Caracciolo, 2020; Liu et al., 2020; Mohammad et al., 2020). Consequently, comprehension and evaluation of the factors's effect on heavy mineral composition are the prerequisite for data interpretation and provenance analysis.

These uncertainties can be minimized or avoided by integrating diverse methods, thus to acquire complete characterization of the sediments (Nie and Peng, 2014). For this reason, a fast and reliable provenance analysis technology is required. However, the important limitations of optical method are time-consuming, laborious and dependent on the experience and subjectivity of the operator (Weltje and von Eynatten, 2004;

Nie et al., 2013; Nie and Peng, 2014; Dunkl et al., 2020). The TESCAN Integrated Mineral Analyzer (TIMA) platform is an integration of scanning electron microscopy-energy dispersive spectroscopy (SEM-EDS) chemical analysis with mineral automated identification software, and consequently particle-by-particle quantitatively determines the mineralogical composition of sediments in multidisciplinary research (Hrstka et al., 2018; Ward et al., 2018; Honeyands et al., 2019). This rapid scanning technique (about 100,000 mineral grains being analyzed per hour) reports quantitative mineral data as well as textural and chemical information on statistically significant samples (Ward et al., 2018), and the applications in Quaternary research includes sediment provenance and tectonic setting (Nie and Peng, 2014; Zhang et al., 2015), weathering and recycling history (Nie et al., 2013), stratigraphic division and sedimentary environment (Haberlah et al., 2010), etc.

The Songhua River, the most important river in Northeast China, has two headwaters (Xie et al., 2020), the Nenjiang River (generally as a tributary to the Songhua River, originating from the Great Hinggan Mountains) and the Second Songhua River (hydrologically as the source of the Songhua River trunk stream, originating from the Changbai Mountains; **Figure 1**). The lithology of the Great Hinggan Mountains is dominated by granitoid, intermediate-acid volcanic rocks and a few basaltic rocks, while the lithology of Changbai Mountains is characterized

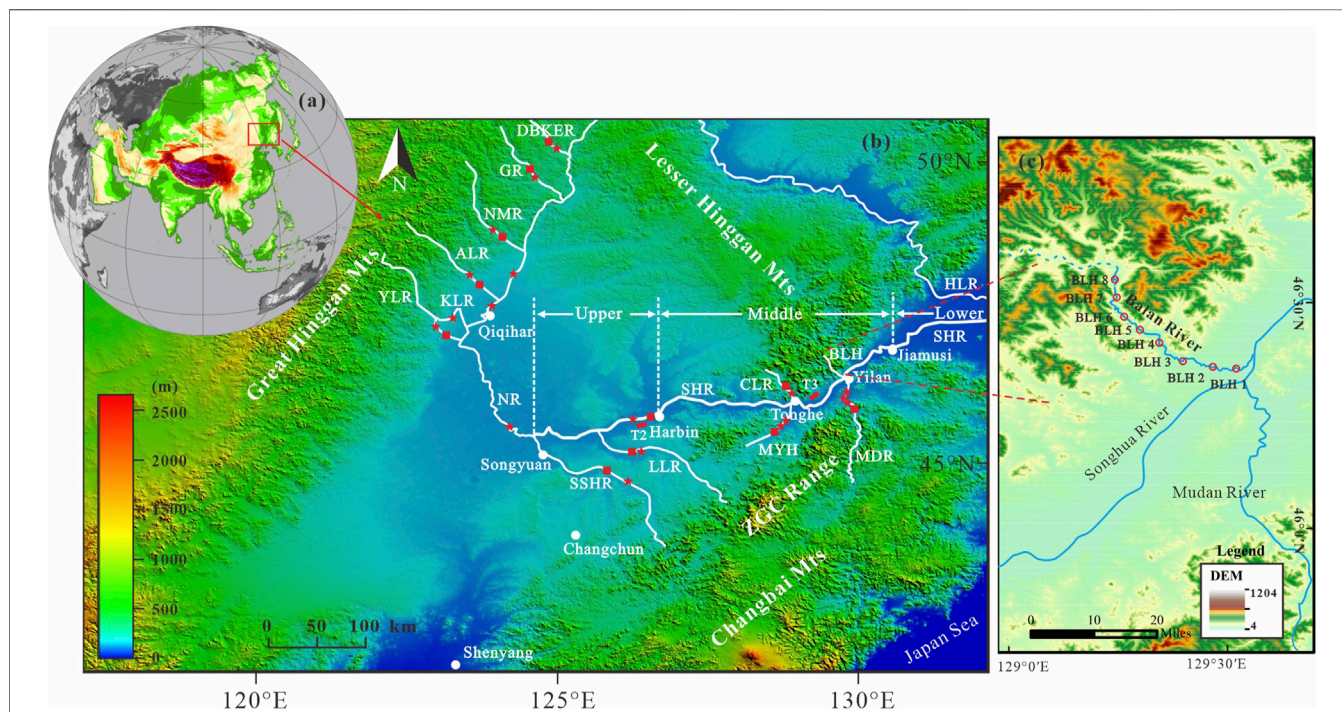


**FIGURE 1 | (A,B)** DEM map of Northeastern Plain, showing the distribution of the Songhua River and Liaohe River drainage system. The red five-pointed stars and squares along the major mainstem and tributaries represent the sample sites used in this study for different grain-size (63–125  $\mu\text{m}$  and 125–250  $\mu\text{m}$ ) and wide grain-size window (63–250  $\mu\text{m}$ ) heavy mineral analysis, respectively. The red filled rectangle represent the fluvial terrace site. **(C)** DEM map of the Balan River, showing the intensive sampling sites for the eight samples. Abbreviation: HLR = Heilong River; NR = Nenjiang River; SHR = Songhua River; SSHR = Second Songhua River; LLR = Lalin River; CLR = Chalin River; MYR = Mayan River; BLH = Balan River; MDR = Mudan River; DBKER = Duobukuer River; GR = Ganhe River; NMR = Nuomin River; ALR = Alun River; YLR = Yalu River; KLR = Kule River; ZGC Range = Zhangguangcai Range. (For interpretation of the references to colour in this figure legend, the reader is referred to the web version of this article.)



The Songhua River drains a variety of orogenic belts and terraces with markedly different geological history. The lithology of the mountains around the Songnen Plain is mainly characterized by intrusive rocks and volcanic rocks, accounting for more than 80% of the outcropped bedrock. The intrusive rocks are mainly granitoid and migmatitic granitoid, and the volcanic rocks are mainly basalt, andesite, rhyolite, intermediate-acid tuff and tuffaceous lava (Song et al., 1986; Fu et al., 2019). The lithology of the Great Hinggan Mountains is mainly characterized by granitoid, intermediate-acid volcanic rocks and a small amount of basalt distributed in the western Great Hinggan Mountains (**Figure 2**). The lithology of the Lesser Hinggan Mountains, the Changbai Mountains and the Zhangguangcai Range is characterized by granitoid, migmatitic granitoid, basalt and Precambrian metamorphic rocks (**Figure 2**). Quaternary loose sediments (e.g., loess, sub-clay, clayey silt, sand and gravel) are widely distributed in the Songnen Plain and the Sanjiang Plain. Climatically, the Songnen Plain is in the northern margin of the East Asian summer monsoon zone, and a transition zone from semi-arid and semi-humid toward semi-arid.

The Songhua River (length 2,309 km, catchment area  $56.12 \times 104 \text{ km}^2$ ), the seventh largest river in China, generally has two headwaters (Zheng et al., 2015), the Nenjiang River (north headwater, originating from the Great Hinggan Mountains) and the Second Songhua River (southern headwater, originating from the Tianchi Lake in the Changbai Mountains; **Figure 1**). Hydrologically, the Nenjiang River generally acts as a tributary to the Songhua River and the Second Songhua River as the source of the Songhua River trunk stream. The Songhua River trunk stream, extending eastward from Songyuan to Tongjiang and finally joining the Heilong River (**Figure 1**), is commonly divided into upper, middle, and lower reaches at Harbin and Jiamusi (Xie et al., 2020). The upper reach (length: 240 km), from Songyuan to Harbin, joined by the Second Songhua River and the Lalin River at its right bank, drains the southeastern part of the catchment. The Chalin River at the left bank and the Mayan River and the Mudan River at the right bank, drain the eastern part of the catchment and are part of the middle reach (from Harbin to Jiamusi, length: 432 km). The lower reach (length: 267 km), from Jiamusi to Tongjiang, drains the Sanjiang Plain and finally joins the Heilong River (**Figure 1**). The Balan River, a case of discussion in this study, is a tributary of the middle reaches of the Songhua River, originates from the Lesser Hinggan Mountains, and has a length of 108 km and a total drainage area of about  $2075 \text{ km}^2$ , with few tributaries (**Figure 1C**).

The Songhua River basin is mainly in the temperate monsoon zone with the same period of rain and heat. The average annual precipitation in the basin is 500–600 mm, and the seasonal distribution is uneven, with summer (June–August) rainfall accounting for 70%–80% of the year. In winter, all the rivers in the basin have icing periods (November–April), with icing periods of 130–180 days. The flow velocity of the Harbin section of the Songhua River varies little, between 0.536 and 1.99 m/s (HLCC (Harbin Local Chronicles Committee), 1993). The annual average runoff of the main stream of the Songhua River, Nenjiang River and Second Songhua River is 1180, 685 and  $483 \text{ m}^3/\text{s}$ , respectively. The floods in Harbin segment are caused by a

combination of water from the Nenjiang River, the Second Songhua River and the Lalin River, of which Nenjiang River accounts for about 60%, the Second Songhua River and Lalin River for 30% and 10% respectively (HLCC (Harbin Local Chronicles Committee), 1993). Influenced by the confluence of upstream tributaries and reservoirs, the flood process in the main stream of Songhua River (Harbin section) lasts for a long time, usually taking about 7–21 days, with the annual average maximum flood flow reaching  $4,000 \text{ m}^3/\text{s}$  (HLCC (Harbin Local Chronicles Committee), 1993).

Just for clarity, the Songhua River drainage in this study will be divided into three parts, the Nenjiang River reaches (including the trunk stream of the Nenjiang River and its main tributaries), the upper reaches of the Songhua River (including the Second Songhua River, the Lalin River and the trunk stream of the Songhua River from Songyuan to Harbin) and the middle reaches of the Songhua River (including the trunk stream of the Songhua River from Harbin to Jiamusi and its main tributaries), to facilitate comparative analysis.

## SAMPLING AND ANALYTICAL METHODS

### Sampling

In this study, a total of 32 modern river sand samples were taken, at the depth of 20 cm below the surface for avoiding contamination by human activity, from point bar of the mainstream and major tributaries of the Songhua River system. Among them, 21 samples were performed for multi-window analysis ( $63\text{--}125 \mu\text{m}$  and  $125\text{--}250 \mu\text{m}$ ), using conventional optical methods, and the other samples were selected for both conventional optical and TIMA analysis, at a wide grain-size window ( $63\text{--}250 \mu\text{m}$ ), in order to compare application of the methods to heavy mineral analysis and to further evaluate the application of wide-window and multi-window strategies to heavy-mineral interpretation.

To assess the influence of fluvial transport-deposition processes on heavy mineral composition, a total of eight river sand samples from point bar of the Balan River were systematically collected, from upstream to downstream, for multi-window analysis ( $<63 \mu\text{m}$ ,  $63\text{--}125 \mu\text{m}$  and  $125\text{--}250 \mu\text{m}$ ) by conventional optical methods, with a sampling river length of 42 km and height difference of 80 m (**Figure 1B**). In addition, to assess the effect of chemical weathering on heavy mineral composition, two samples from the Songhua River T3 river terrace in Tonghe county (the middle reaches of the Songhua River) and 1 sample from T2 river terrace in Harbin city (the upper reaches of the Songhua River) were collected for multi-window analysis, using conventional optical methods (**Figure 1B**).

### Optical Heavy Mineral Analysis

The samples were dry-sieved to separate the  $<63 \mu\text{m}$ ,  $63\text{--}125 \mu\text{m}$ ,  $125\text{--}250 \mu\text{m}$  and  $63\text{--}250 \mu\text{m}$  fractions. The sub-samples were weighed after drying in the oven with a temperature lower than  $60^\circ\text{C}$ , and then were elutriated repeatedly with clear water and then separated with bromoform (density = 2.88) to collect heavy

minerals. The collected heavy minerals were further separated into ferrimagnetic, paramagnetic and diamagnetic groups using isodynamic separator and then weighed separately again. The heavy mineral groups were identified under stereomicroscopy and polarized microscope, with identification numbers of each mineral species totaling up to 1000 grains. The percentage of heavy minerals was calculated based on the weight. Details for heavy mineral analysis are described in **Supplementary Text S1**.

### TESCAN Integrated Mineral Analyzer Heavy Mineral Analysis

The samples were processed into thin sections for heavy analysis using the TIMA SEM-EDS system. TIMA works by generating a backscattered electron image (BSE) and Energy Dispersive X-ray (EDX) from a thin section to identify individual mineral particles. Multiple EDX detectors scan each mineral particle at a predetermined resolution (pixel spacing). The resulting EDX spectrum is automatically analyzed according to the TIMA classification scheme and a specific mineral phase is assigned to each particle from the mineral definition file, thereby generating an accurate mineralogical map for each mineral particle. The TIMA technology provides the length and width of each particle by mineral phase-specific grain size analysis. The grain size intervals to be analyzed can be exported *via* offline software once the mineral target scan is completed.

The TIMA analysis was operated using high-resolution liberation mode, and conducted at operating conditions of 25 keV using a spot size of 69.61 nm, a working distance of 15 mm and a field size set at 1,500  $\mu\text{m}$ . The image and grain resolution is determined by the pixel spacing, here with 2  $\mu\text{m}$  pixel size. After the tests are completed, the TIMA offline processing software is used to obtain the test point spectra. Element identification is automatically performed and the content of the identified elements is calculated based on the characteristic energy values of the test point spectra. The spectral lines and the elemental content of the test point are then compared with the spectral lines and composition of standard or existing minerals in the database to determine the mineral type and name of the test point (Hrstka et al., 2018; Chen et al., 2021). Finally, various data analysis reports are exported as needed. The detailed operating steps are described in **Supplementary Text S2**. The pretreatment, mineral separation and identification were all carried out at the Chengxin & Chengpu geological Testing Co. Ltd, Langfang, China.

### Petrography Analysis

In order to further identify the weathering of the river terrace samples, four bulk samples selected from the Songhua River T3 river terrace in Tonghe county were directly made to 30  $\mu\text{m}$  thick standard thin sections for traditional petrographic study. These thin sections were observed under a polarizing microscope and with a focus on the alteration characteristics of the minerals. The point-counting spacing interval was constant for each thin section and was dependent on the sizes of major crystals in the analyzed samples.

## RESULT

### Heavy Mineral Composition in the Upper Reaches of the Songhua River

A detailed heavy mineral composition of the 63–125  $\mu\text{m}$  and 125–250  $\mu\text{m}$  is listed in **Supplementary Tables S1, S2**, respectively. In 63–125  $\mu\text{m}$  fraction, amphibole is the dominant heavy mineral representing 37.63%–65.42% of the heavy mineral assemblages, and epidote and ilmenite comprise 5.18–25.87% and 5.72–16.14%, respectively (**Figure 3**). Apatite, sphene, granet, hematite-limonite, ferromagnetic minerals (magnetite and maghemite) and ultrastable minerals (e.g., zircon, tourmaline and rutile) occur in different percentages. Both anatase and leucoxene are occur only in traces, and pyroxene is absent in the Second Songhua River (**Figure 3**). In comparison to the 63–125  $\mu\text{m}$  samples, the 125–250  $\mu\text{m}$  fraction has the same heavy mineral species with decreasing concentration except for amphibole and epidote (**Figure 3**). The T2 fluvial terrace of the Songhua River is dominated by the unstable minerals amphibole (34.89%) and epidote (25.54%) in both size fractions (63–125  $\mu\text{m}$  and 125–250  $\mu\text{m}$ ) and is roughly similar to the heavy mineral composition of modern fluvial sands of the Songhua River (**Figure 3**).

### Heavy Mineral Composition in the Middle Reaches of the Songhua River

For 63–125  $\mu\text{m}$  fraction, amphibole (22.12%–64.23%) is the most frequent heavy mineral, followed by ilmenite (4.33%–23.72%), sphene (3.66%–16.35%), ferromagnetic minerals (1.29%–22.16%) and epidote (3.04%–21.00%); the other heavy minerals, including hematite-limonite, granet, ultrastable minerals, leucoxene, apatite and pyroxene, occur in small amounts (0.1%–4%); anatase is found in trace amounts (<0.1%); monazite, tremolite and siderite are occasionally present. The contents of sphene and amphibole in 125–250  $\mu\text{m}$  fraction samples increase compared with 63–125  $\mu\text{m}$  fraction, while the contents of other minerals decrease to different degrees (**Figure 3**).

The heavy mineral assemblages of the T3 terrace in Tonghe are significantly different from those of the stream samples. The unstable minerals (e.g., amphibole, pyroxene) and moderately stable minerals (e.g., sphene) almost disappear, while the stable minerals (e.g., ilmenite) and ultrastable minerals are significantly enriched (**Figure 3**).

### Heavy Mineral Composition in the Nenjiang River Reaches

In 63–125  $\mu\text{m}$  fraction, heavy mineral assemblages are dominated by epidote (25.16%–38.52%), ilmenite (5.68%–27.77%), hematite-limonite (2.21%–31.98%), amphibole (1.14%–24.59%) and sphene (3.66%–15.54%); apatite, granet, anatase, leucoxene and ultrastable minerals are rare or absent in most sub-samples (**Figure 3**); pyroxene content in the Nuomin River is the highest in the entire Songhua River drainage. The 125–250  $\mu\text{m}$  fraction is marked by the obvious increase of epidote and amphibole compared to the 63–125  $\mu\text{m}$  fraction (**Figure 3**).

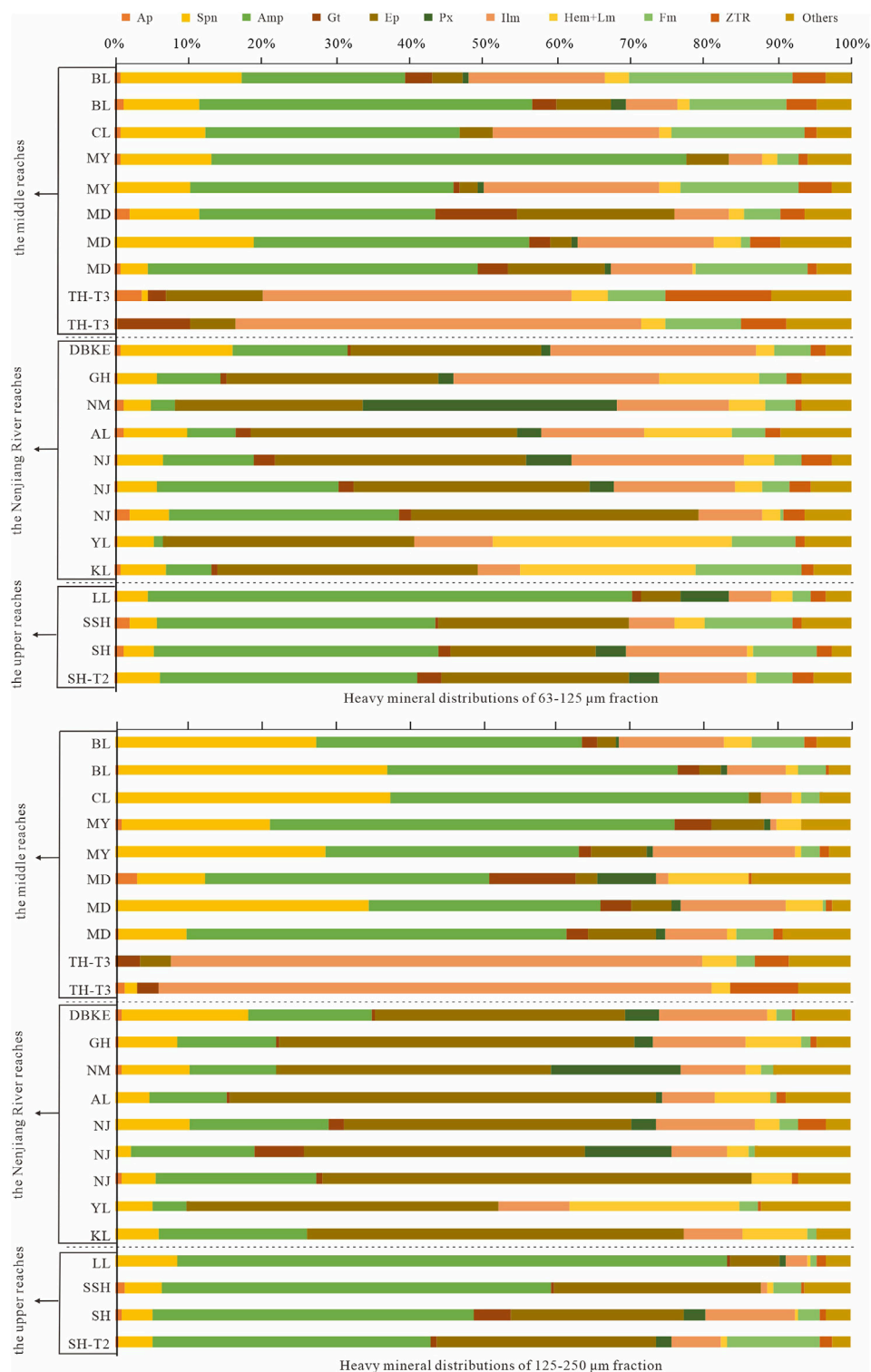
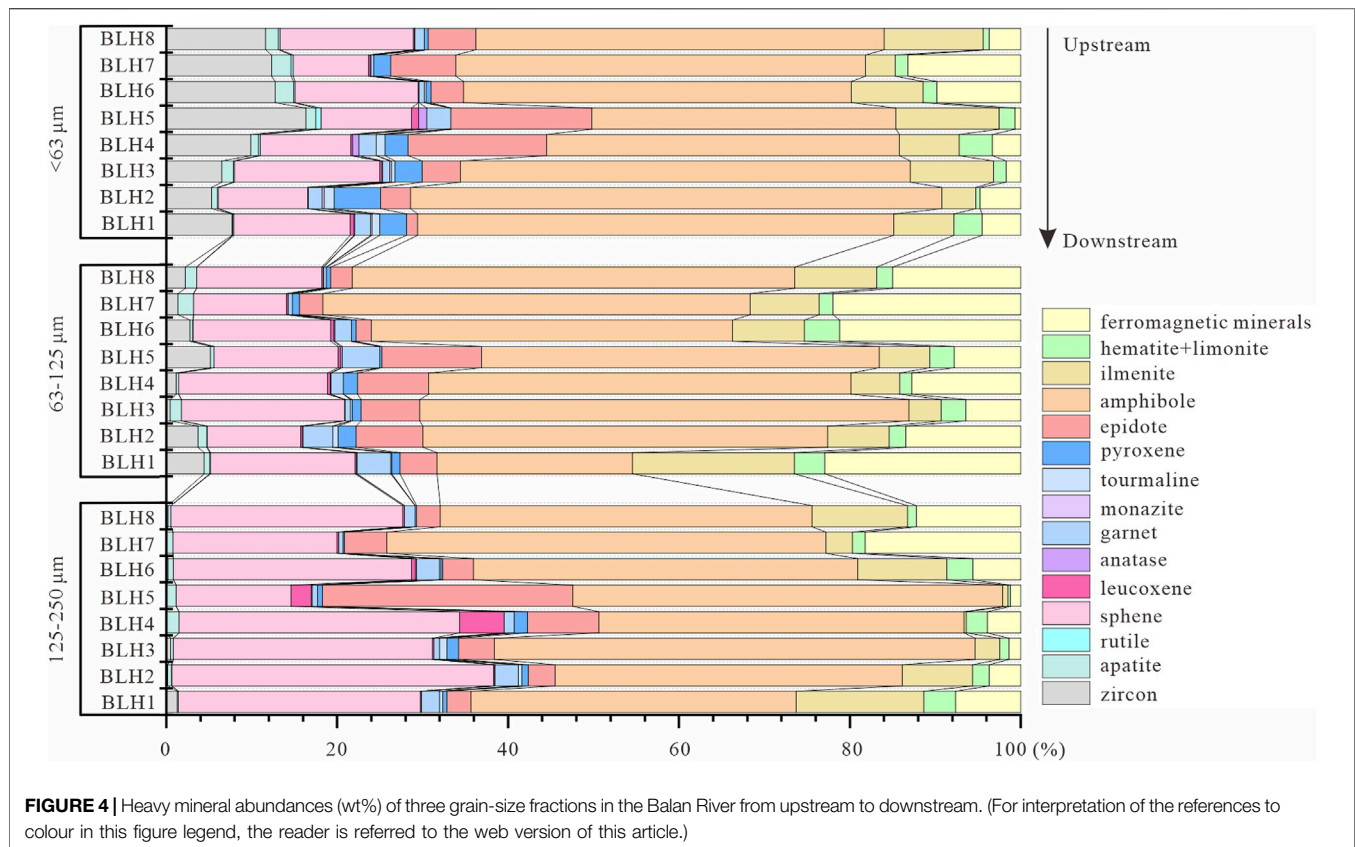


**FIGURE 3 |** Heavy mineral abundance of the Songhua River at 63–125  $\mu\text{m}$  and 125–250  $\mu\text{m}$  fraction, expressed as relative weight percentage (wt%). Systematic mineral abbreviation list: Ap = apatite, Spn = sphene, Amp = amphibole, Gt = garnet, Ep = epidote, Px = pyroxene, Ilm = ilmenite, Hem = hematite, Lm = limonite, Fm = ferromagnetic minerals, ZTR = zircon + tourmaline + rutile. (For interpretation of the references to colour in this figure legend, the reader is referred to the web version of this article.)



## Heavy Mineral Composition in the Balan River

The heavy mineral results of the Balan River were shown in **Figure 4** and **Supplementary Table S4**. In the <63  $\mu\text{m}$  fractions, amphibole (30.75%–55.97%), sphene (8.23%–15.81%) and zircon (4.76%–14.11%) are absolutely dominant, monazite only occurs stably in the downstream, and other minerals occur in different proportions. In comparison, amphibole (22.12%–50.50%), ferrimagnetic minerals (6.17%–22.16%) and sphene (10.50%–18.37%) are the main minerals in the 63–125  $\mu\text{m}$  fraction, with a dramatic decrease in zircon content; in the 125–250  $\mu\text{m}$  fraction, sphene (12.04%–35.97%) and epidote (2.71%–26.21%) gradually increase, and zircon and monazite almost disappear.

## Heavy Mineral Composition by the TESCAN Integrated Mineral Analyzer and Optical Method

The 12 representative samples were carried out for heavy mineral analysis using both optical and TIMA method. The BSE, scanning electron images and mineral phase maps are shown in **Supplementary Figure S1**. Based on 15,000 to 25,000 grain counts per sub-sample, the TIMA data report the same heavy mineral results as the optical. However, the TIMA results identify more types of mineral species (**Supplementary Table S3**). In

order to facilitate comparison with optical results, we have combined similar minerals (**Figure 5**). The major differences between the two methods are the more abundant epidote and  $\text{TiO}_2$  group minerals (e.g., rutile, anatase and brookite) and disappearing anatase phase in TIMA results (**Figure 5**).

## Petrographic Characteristics in the Tonghe T3 River Terrace Sediments

The T3 river terrace sediments are mainly composed of quartz, feldspar, mica and debris (**Figure 6**). Quartz is characterized by sub-angular/sub-round, colorless transparent, wavy extinction and obvious corrosion in grain edge (**Figure 6**). Feldspar is strip, irregular granular. Most of k-feldspar underwent clayization alteration, with a small amount of sericitization alteration. Plagioclase has polysynthetic twin, sericitization and clayization alteration (**Figure 6**). Mica is flake and parallel extinction. The debris are irregular in shape and is 0.05–1.00 mm in size (**Figure 6**). Clay minerals in YL-13 sample are brownish-yellow in colors and exist as fillings (**Figure 6C**).

## DISCUSSION

Heavy mineral method is one of the most favorite tools for tracing the source of clastic sediments (Morton and Hallsworth, 1999;

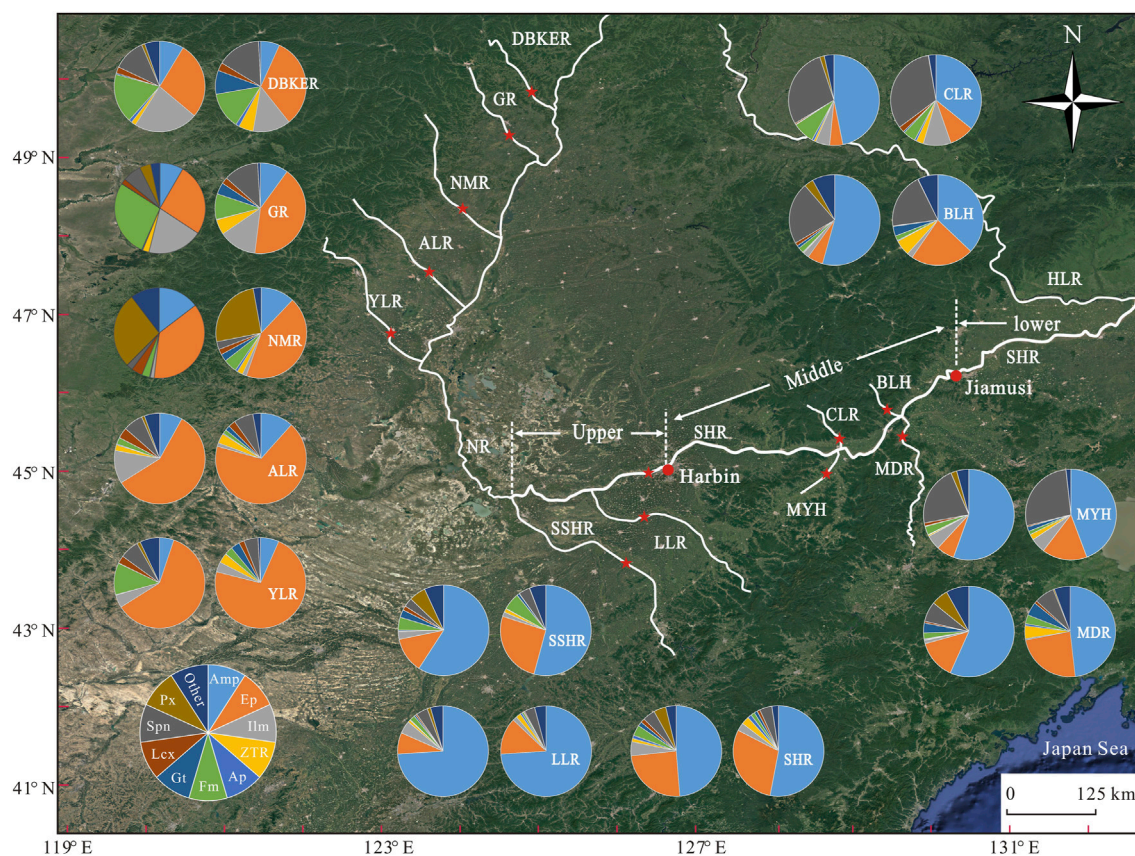


**FIGURE 5** | A comparison composition of heavy mineral assemblages of the Songhua River based on the traditional optical (left) and TIMA (right) methods. Note that more abundant epidote and ZTR minerals in TIMA results. Abbreviation definitions see **Panels 1, 3**. (For interpretation of the references to colour in this figure legend, the reader is referred to the web version of this article.)

Morton and Hallsworth, 2007). However, the autogenic and external forcing (e.g., lithology, hydrodynamic sorting, chemical weathering, mechanical breakdown, diagenesis dissolution and sedimentary process) collectively control the composition of clastic sediments, potentially resulting in compositional biases and erroneous interpretations if they are not taken into consideration (Caracciolo, 2020). In this section we take heavy mineral composition in the Songhua River drainage system as an example to clarify the effect of limiting factors (provenance, transport processes and chemical weathering) on heavy mineral composition, and then to evaluate the application of TIMA and conventional optical methods.

## Provenance

There are three main parent sources of the drainage networks in the Songnen Plain, namely the Great Hinggan Mountains in the northwest, the remnants of the Changbai Mountains in the southeast and the Lesser Hinggan Mountains in the northeast (**Figure 1**). The Great Hinggan Mountains are mainly granitoid and intermediate-acid igneous rocks in lithology, with a small amount of basalt, gabbro and other basic rocks. The Lesser Hinggan Mountains, the Changbai Mountains and the Zhangguangcai Range are characterized by granitoid,

migmatitic granitoid, basalt and Precambrian metamorphic rocks (**Figure 2**).

Distinct mineral assemblages are typically associated with the lithology of source rocks, e.g., igneous, metamorphic and sedimentary rocks generating different types of mineral and hence controlling mineral assemblages (von Eynatten et al., 2012; Caracciolo et al., 2015; von Eynatten et al., 2016; Caracciolo, 2020). The tributaries of the Songhua River, with different source areas (i.e., the Great Hinggan Mountains, the Lesser Hinggan Mountains and the Changbai Mountains), have distinctly different heavy mineral composition. For example, the rivers originating in the Great Hinggan Mountains, e.g., the Alun River, the Nuomin River, the Gan River, the Duobukuer River and the Yalu River, have very high epidote (>25%) and very low amphibole (<15%) and moderately high leucoxene content (>1.8%), while the rivers originating in the Lesser Hinggan Mountains, e.g., the Balan River and the Chalin River, have very high sphene content (>20%; **Figure 3**).

Although the source parent rocks surrounding the Songnen Plain are predominantly intermediate-acid magmatic rocks, locally exposed basal rocks and other metamorphic and sedimentary rocks make the tributaries flowing through different parent rock areas have significantly different heavy

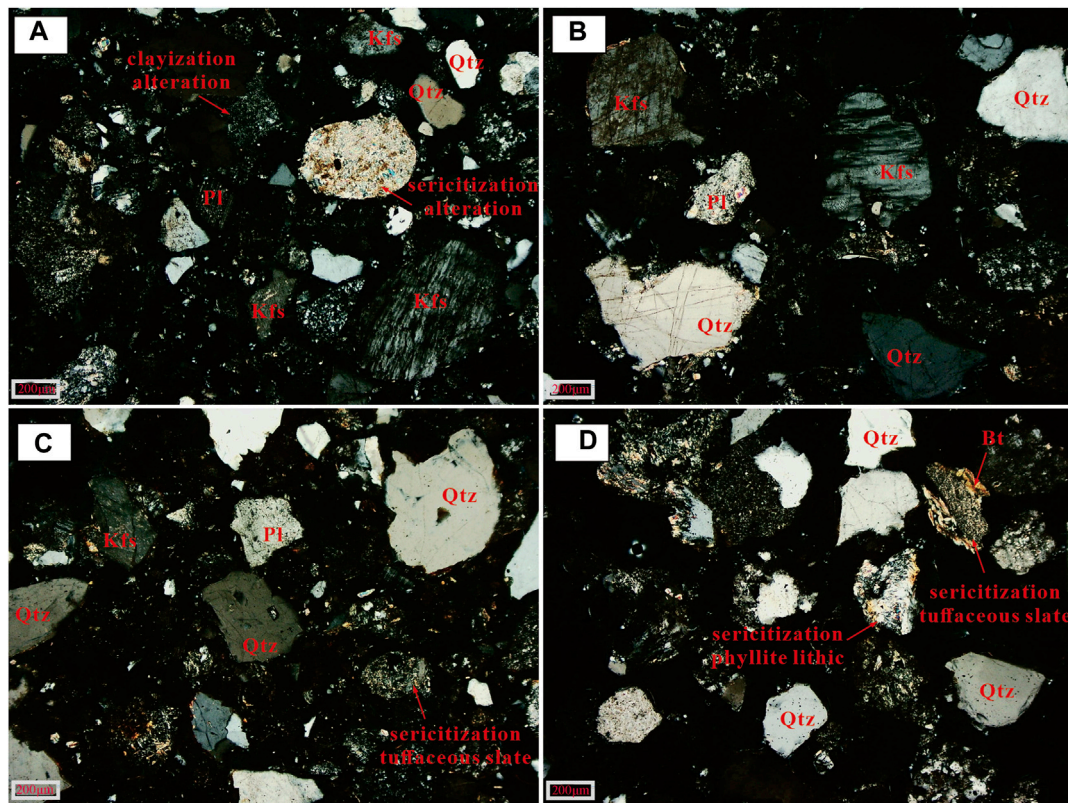


**FIGURE 6** | Thin section photomicrographs of the samples of Tonghe T3 fluvial terrace (Qtz = quartz; Kfs = K-feldspar; Pl = plagioclase; Bt = biotite). Note that both K-feldspar and plagioclase show sericitization and clayization alteration to varying degrees, and the edge of quartz shows dissolution characteristics.

mineral composition. For example, the tributaries of the Nenjiang River, which originate in the Great Hinggan Mountains, are featured by substantially high content of pyroxene (Nuoming River), ilmenite (Gan River, Duobukuer River and Alun Rivers) and hematite + limonite (Gan River, Duobukuer River, Yalu River and Kule River) (Figure 3), which indicates the dominant control of basic parent rocks on heavy mineral composition, as recorded by significantly existing basal rocks in modern riverbed gravels. Large areas of basalt rocks are exposed in the upper-middle reach of the Nuomin River (Figure 2), reasonably explaining the marked enrichment of pyroxene phase in the Nuomin River sediments.

## Sorting

Controlled by the gravity and flow physics laws, sediment particles are usually separated into different fractions during the river “source-to-sink” process (Caracciolo, 2020). Hydrodynamic conditions as well as differences in grain size and density of minerals will result in the enrichment or absence of minerals in particular fraction (e.g., Krippner et al., 2015; Krippner et al., 2016; Vezzoli et al., 2016). For instance, the catchment area draining the Almklovdalen peridotite massif in SW Norway reveals that MgO-rich almandine garnets are more frequent in the coarser grain-size fractions, whereas MnO-rich almandine garnets are more frequent in the finer grain-size

fractions (e.g., Krippner et al., 2016). Therefore, single-mineral provenance analysis may also be unreliable if the hydrodynamic behavior of heavy minerals is not adequately considered (e.g., Lawrence et al., 2011).

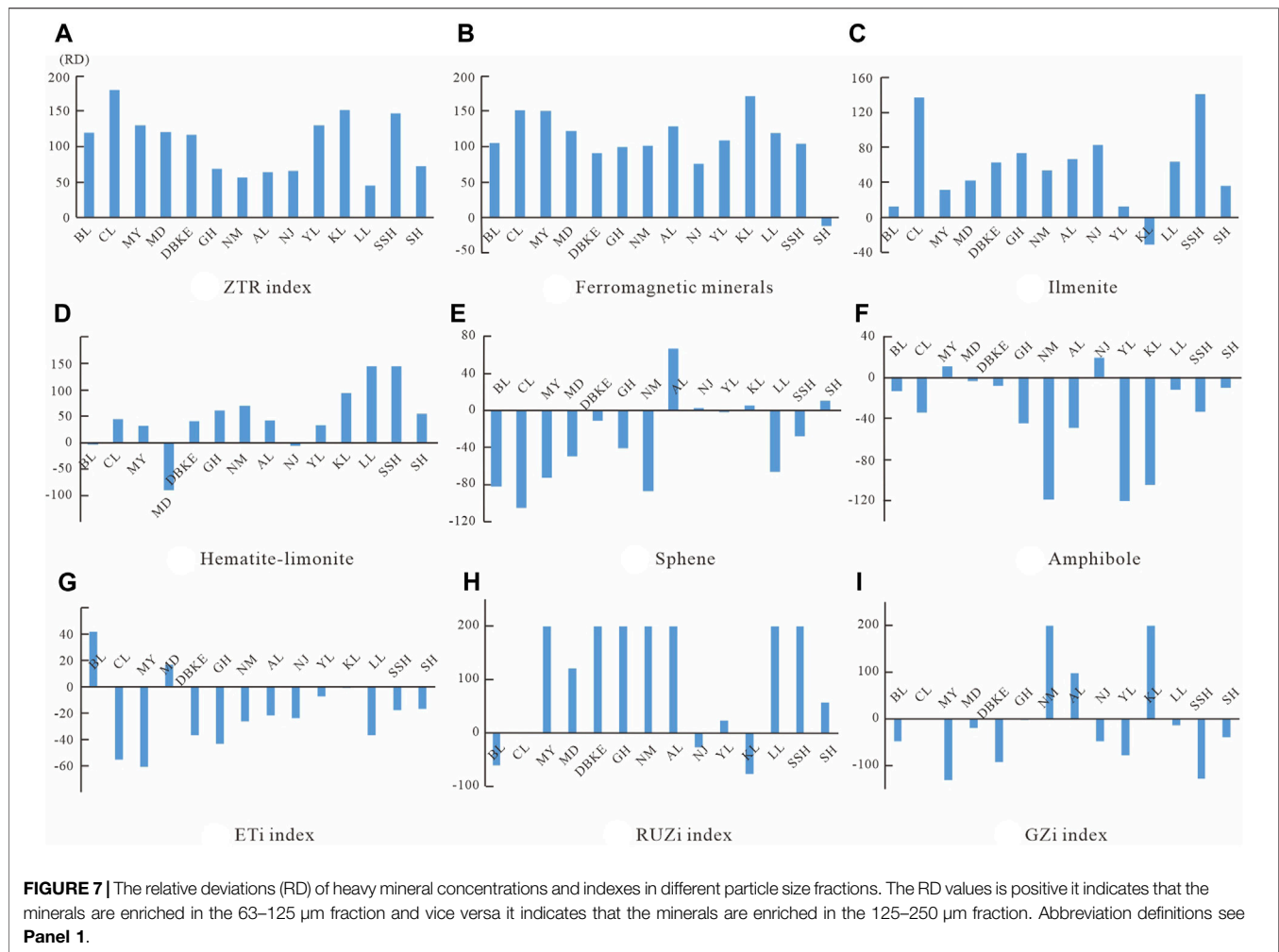
The relative deviations (RD) of heavy mineral concentrations in different particle size fractions can be calculated by the following equation (Yang and Li, 1999):

$$RD = \frac{C_a - C_b}{C_a + C_b} \times 200$$

Where  $C_a$  and  $C_b$  is the average mineral content in the 63–125  $\mu\text{m}$  and 125–250  $\mu\text{m}$  fraction, respectively. When the RD value  $> 0$ , it indicates that the minerals are enriched in the 63–125  $\mu\text{m}$  fraction, and inversely, the minerals are enriched in the 125–250  $\mu\text{m}$  fraction.

The RD calculation results are illustrated in Figures 7A–F. The ZTR (zircon + tourmaline + rutile) minerals, ferrimagnetic minerals, ilmenite and hematite-limonite in the studied sediments are enriched in the 63–125  $\mu\text{m}$  fraction, while sphene and amphibole are relatively enriched in the coarser 125–250  $\mu\text{m}$  fraction, which shows the marked effect of hydrodynamic separation on the heavy mineral composition.

Grain-size window strategy for heavy mineral analysis is considered to reduce or eliminate potential hydrodynamic



sorting effects. Although the majority of heavy minerals are likely to be concentrated in the 63–125  $\mu\text{m}$  fraction, the strategy of reducing the impact of hydrodynamic sorting by narrowing the grain-size window is still unwise, as this is likely to provide an average source signal and may ignore the contribution from relatively barren lithologies (Garzanti and Andò, 2007; Garzanti et al., 2008). Previous studies have demonstrated that broadening the grain-size window can avoid misleading interpretations for provenance signatures (e.g., Krippner et al., 2016). For instance, Garzanti et al. (2006) showed that it is possible to distinguish the provenances of the different tributaries of the Nile River only when considering the 40–500  $\mu\text{m}$  grain-size range, due to the enrichment of amphibole in the coarser sediments. A wide-window strategy that is significantly wider than the grain-size spectrum of all minerals, is supposed to can yield unbiased information. However, the strategy results in a greater number of fine-grained but denser heavy mineral grains being involved, making the volume percentages of denser minerals systematically overestimated (Galehouse, 1971; Garzanti et al., 2009). As such, a multi-window strategy, which emphasizes the

determination of two or more grain-size windows to produce unbiased information, has been proposed for heavy mineral analysis (Garzanti et al., 2009).

In this study, the wide window (63–250  $\mu\text{m}$ ) and the multi-window (63–125  $\mu\text{m}$  and 125–250  $\mu\text{m}$ ) of the Songhua River drainage sediments differed significantly in the dominant heavy mineral assemblages. Specifically, the dominant heavy mineral assemblages in the upper reaches of the Songhua River are (Amp + Ep), (Amp + Ep + Ilm + Fm) and (Amp + Ep + Spn + Ilm/Fm) at 63–250  $\mu\text{m}$ , 63–125  $\mu\text{m}$  and 125–250  $\mu\text{m}$  fraction, respectively (**Supplementary Table S5**). Similarly, the dominant heavy mineral assemblages in the middle reaches of the Songhua River drainage sediments are (Amp + Spn + Ep), (Amp + Spn + Ilm + Fm) and (Amp + Spn + Ilm) at 63–250  $\mu\text{m}$ , 63–125  $\mu\text{m}$  and 125–250  $\mu\text{m}$  fraction, respectively (**Supplementary Table S5**). Importantly, eight samples from the Balan River also show the significantly distinct heavy mineral composition in three grain-size fractions (**Figure 4**). For example, the content of zircon, apatite and rutile decreases significantly when the sediment particles become coarser, whereas pyroxene shows an enrichment in coarser grains

(Figure 4). Some minerals show unique enrichment patterns, e.g., monazite occurs stably only in the fine-grained (<63  $\mu\text{m}$ ) fraction, and ferromagnetic minerals reach a maximum in the 63–125  $\mu\text{m}$  fraction (Figure 4). In conclusion, the heavy mineral composition of the different grain-size window in the Balan River further indicates the important influence of sorting during fluvial processes. In this scenario, the multi-size window strategy provides a complementary dominant heavy mineral assemblages, thus providing more complete and accurate information on heavy minerals.

Notably, our data show that the amphibole and sphene contents are systematically overestimated in the wide window, resulting in a simplistic heavy mineral assemblage (Figure 3 and Supplementary Figure S2). The grain-size dependency of heavy minerals in river sediments can be explained by the principle of settling-equivalence (Rubey, 1933; Garzanti et al., 2008; Garzanti et al., 2009; Caracciolo, 2020). This principle states that coarser sized, lower density minerals settle at the same rate as finer sized, higher density minerals. In general, denser minerals are concentrated in the fine tail of the sorted sediment and, conversely, less dense minerals are concentrated in the coarse tail of the sorted sediment (Komar and Wang, 1984; Garzanti et al., 2009). Therefore, some mineral contents may be systematically overestimated in wide-window strategy due to the effect of settling-equivalence. Thus, our results provide new evidence that a multi-window strategy for analyzing each particle size range of each sample individually is an more effective way to obtain complete heavy mineral information in source areas than a fixed wide or narrow size window, despite the fact that this may be time-consuming.

A series of heavy mineral ratios consisting of minerals with similar density, diagenetic and hydraulic behavior are believed to can effectively avoid the effects of grain-size sorting and diagenesis, e.g., ATi, GZi, RuZi, ETi, MZi and CZi index (Morton and Hallsworth, 1994; Morton and Hallsworth, 1999). Nevertheless, we still need to evaluate the extent to which these indices can avoid grain-size sorting effects before they are used. The RD values of the indices indicate that the indices in this study are clearly influenced by the particle size sorting effect (Figure 7). The RD values of the ETi index are almost always negative, indicating that the ETi index has a higher value in the 125–250  $\mu\text{m}$  fraction (Figure 7G). As a comparison, the RuZi index presents higher values in the fine-grained fraction (Figure 7H). In addition, the RD values of the GZi index show a relatively complex distribution pattern, e.g., the GZi index presents high values in the 63–125  $\mu\text{m}$  fraction in the Nuomin River, Alun River and Kule river, while this is not the case for the other rivers (Figure 7I). In this case, caution should be exercised when investigating weathering and recycling history, provenance and tectonic setting based on heavy mineral characteristic indices.

## Fluvial Transport-Depositional Processes

Fluvial sediments are thought to faithfully record the characteristic components representing the lithologic assemblage of the catchment, yet the source area signal exhibits significant complexity as it propagates downstream

(Jackson et al., 2019). For this study, just as an example, some high contents of diagnostic minerals specific to the tributaries of the Nenjiang River, e.g., epidote, pyroxene, ilmenite and hematite + limonite, are of very low content in the Nenjiang River and especially the Songhua River trunk stream. Specifically, epidote, a dominant mineral phase in the tributaries of the Nenjiang River, holds a poor content in the Songhua River trunk stream in which amphibole is dominant mineral phase (Figure 3); the Nuomin River is dramatically enriched in pyroxene phase (34.29%) due to it is drainage through the basaltic zone (Figure 2), and however, after it joins the Nenjiang River, the pyroxene content decreases strongly downstream (i.e., 6%, 3.18% and 0% in the Nenjiang River samples; Figure 3); in addition, the other unique fingerprints of the tributaries of the Nenjiang River, e.g., the high content of ilmenite in the Ganhe River and the Duobukuer River, and of hematite-limonite in the Yalu River and the Kule River (Figure 3), have been significantly blurred and even disappeared in the Songhua River trunk stream (Figure 3). The very weak parent-rock information of the Great Hinggan Mountains in the trunk stream of the Songhua River indicates that the source control on heavy mineral composition is influenced by fluvial processes. Therefore, a downstream dilution eventually creates a compositionally stable mixture and reflects the average volumetric contribution of the lithological assemblage, thus obscuring the provenance signal of the locally exposed parent rocks in the upstream (e.g., Weltje, 2012; Krippner et al., 2016; Caracciolo, 2020).

It is essential to note that the clear downstream decrease in the diagnostic minerals in the tributaries of the Nenjiang River may also be the result of chemical dissolution. Strong chemical weathering can profoundly change the composition of sediments, especially when fluctuating with low-gradient relief (Johnsson and Basu, 1993). It is well known that pyroxene and amphibole are both unstable mineral species and highly susceptible to chemical dissolution (e.g., Morton, 1985; Nie et al., 2013). However, the unstable mineral amphibole and the moderately stable mineral epidote are abundantly present as dominant minerals in the Songhua River sediments (Figure 3), indicating a limited effect of chemical weathering. The weak chemical weathering condition is further supported by the local semi-arid-cold climatic regime and the primary weathering level of the Quaternary loess deposits (e.g., Xie et al., 2018; Wu et al., 2021).

It has recently been proposed based on erosion models in the Yangtze River catchment that even after long-distance transport across vast continental regions, clastic mineral models remain reveal the tectonic characteristics of the source rather than the geodynamic setting of the sink (Vezzoli et al., 2016). However, it remains uncertain whether the specific compositional features found in the lower reaches or inlets of rivers have been interfered by other factors (e.g., dilution and homogenization by river erosion-transportation-sedimentation and recycled processes), after a long-range and long-term transport. The same phenomenon also occurs in the single mineral tracer technology. For example, the U-Pb age distributions along the large Rio Pastaza catchment show a downstream loss of important age populations likely due to pronounced input

from singular sources, leading to dilution of upstream signatures from the hinterland and magmatic arc (Jackson, et al., 2019). In river source-to-sink processes, therefore, some keys must be given attention, such as the specific grain-size interval of sediments that can complete the source-to-sink route, the mixing and dilution of different information carried by the sediments continuously added along the route, etc.

It is interesting to mention that a dramatic variation in the content of certain mineral phases is observed in the different river reach (albeit short distances apart). The eight samples of the Balan River show significant differences in heavy mineral composition in the same grain-size fraction (Figure 4). As an example, the contents of sphene, leucoxene, epidote, ilmenite and ferromagnetic minerals in the samples vary greatly in 125–250  $\mu\text{m}$ , and ultra-stable minerals (e.g., rutile, tourmaline) are present only in individual samples (Figure 4). In addition, the heavy mineral assemblages exhibit diverse characteristics due to the significant differences in heavy mineral content between each sample. Likewise, ilmenite in two samples (4.33% and 23.72%) from the Mayan River and epidote in three samples (3.04%, 12.87% and 21.00%) from the Mudan River also show significant differences (Figure 3). Accordingly, the critical role of river transport processes, regardless of the transport distance, is further confirmed.

In conclusion, considering the effect of fluvial processes on heavy mineral composition, the following points should be considered. First, the composition of heavy minerals depends largely on the particle size, and some minerals in specific size fractions are not lost when multi-size window are used. Second, using only a few samples will introduce an important bias in heavy mineral composition when identifying and quantifying the provenance and detrital contribution from an entire catchment (Vezzoli et al., 2016; Chew et al., 2020). Consequently, a sufficient sample number needs to be considered to obtain a complete picture of heavy mineral composition throughout the entire river system. Finally, the location of sampling sites is equally important. Sites with high-energy flows should be avoided for sampling in modern river systems because they are usually severely damaged by river avulsion processes (Caracciolo, 2020). The best sampling locations are those where laminar flows are dominant hydrodynamic states (e.g., river bars or floodplains), as this minimizes selective sorting of traction flows, resulting in more representative samples (Garzanti, 2019; Caracciolo, 2020).

## Chemical Weathering

In general, due to vulnerability of unstable minerals in sediments to chemical weathering, heavy mineral composition in sediments is largely influenced by chemical weathering process, dependent on the degree of chemical weathering. As such, stable minerals are supposed to be clearly enriched in sediments subjected to moderate-to-high degree of chemical weathering. However, weaker chemical weathering conditions have the opposite behavior (e.g., Morton, 1985; Morton and Hallsworth, 1999; Middleton, 2003; Van Loon and Mange, 2007; Nie et al., 2013).

River terraces, abandoned parts of river channels in the geological past, are important paleo-drainage archives. As

such, the sediments in river terraces have been used to reconstruct drainage evolution and source-sink relations (e.g., Wang et al., 2021). However, our study shows that the heavy mineral characteristics of river terraces with different degrees of weathering differ to varying degrees from modern river sediments (Figure 3). The modern fluvial and T2 terrace sediments of the Songhua River (weak degree of chemical weathering) are dominated by the unstable minerals (e.g., amphibole and epidote) in both size fractions (63–125  $\mu\text{m}$  and 125–250  $\mu\text{m}$ ), with less hematite and ultra-stable minerals, and the contents of apatite, pyroxene and titanite remain largely unchanged (Figure 3). It indicates that the T2 fluvial terrace of the Songhua River has largely retained its heavy mineral characteristics. However, the heavy mineral characteristics of the Tonghe T3 river terrace sediments have been significantly altered relative to the initial time of their deposition. The sediments in the Tonghe T3 river terrace are represented by remarkably high CIA values (the Chemical Index of Alteration,  $\text{CIA} = 83$ , Xie et al., 2020), which indicate an enhanced degree of chemical weathering. In addition, in the petrographic analysis, both K-feldspar and plagioclase show sericitization and clayization alteration to varying degrees, and the edge of hard quartz also shows obvious dissolution characteristics (i.e., the edge is not neat with dissolution pits; Figure 6). Together, these results provide strong evidence for the strong weathering characteristics of the Tonghe T3 terrace sediments.

A comparison of heavy mineral composition in the Tonghe T3 river terrace samples with that of the present fluvial sediments (e.g., the Mayan River and the Chalin River) reveals a remarkably increased content of ZTR index and ilmenite as well as a near disappearance of amphibole and sphene (Figure 3), indicative of a dominant control of heavy mineral composition by chemical weathering rather than by provenance. With this scenario, the use of terrace samples to reconstruct past hydrological evolution or as modern analogues is a matter of discretion.

It is of interest to point out that a recent study in the Yellow River Delta suggests a negligible diagenetic dissolution for the core sediments because of the shallow depth (~200 m) and relatively young ages (~1.9 Myr; Liu et al., 2020). However, a careful assessment of the chemical weathering and diagenesis experienced by sediments is essential before proceeding with the interpretation of the depositional environment and source-sink relations.

## Comparison TESCAN Integrated Mineral Analyzer Scanning Electron Microscopy-Energy Dispersive Spectroscopy Analysis With Optical Method: Advantages and Limitations

Manual statistics of minerals are time-consuming and labor-intensive, and they are susceptible to the subjective factors and knowledge of operators (Ward et al., 2018; Caracciolo et al., 2019). Therefore, automatic mineral identification technology is becoming popular, and provenance tracing of sediments is increasingly becoming automated, quantitative and multi-method analysis (Ward et al., 2018; Dunkl et al., 2020; Xu et al., 2021).

For this study, compared with the manual optical identification, the TIMA method shows a great advantage in identifying mineral species, and more than thirty heavy mineral species (including amphibole group, garnet group and epidote group, etc.) were identified (**Supplementary Figure S1**), which reflects the diversity of minerals in the samples as opposed to the monotonic mineral of traditional optical method. After integrating the same groups of mineral species, however, the TIMA results document heavy mineral assemblages almost identical to those of the optical method (**Figure 5**). Notably, there are still some specific differences. For example, TIMA gives higher ZTR values relative to the optical method (**Figure 5**). Two complementary hypotheses were proposed to explain this phenomenon. During pouring out grains for heavy mineral analysis, the preferential pouring order makes it possible for the ultra-dense particles to be preferentially isolated from the parent sample, causing the ultra-dense particles to be concentrated preferentially in the part that is dumped first (e.g., Zhang et al., 2015). However, the sub-samples used for both analytical methods in this study were separated from the parent sample at the same time and there is no sequential relationship. Therefore, such ultra-dense particles will not be enriched in the sub-samples used for TIMA analysis. Additionally, Previous studies have demonstrated that the SEM-EDS-based QEMSCAN method cannot distinguish between polycrystalline minerals with similar chemical composition (e.g., rutile, anatase and brookite) and thus overestimates the Ti oxide content (e.g., Nie et al., 2013; Zhang et al., 2015). The TIMA results in this study gave higher content of rutile phase relative to the optical method but did not identify anatase (**Figure 5**), indicating that TIMA cannot distinguish Ti oxides.

In addition, TIMA is incapable of distinguishing between hematite-limonite and magnetite. In contrast, in optical analysis, an experienced operator can usually distinguish hematite-limonite from magnetite based on the optical characteristics of the mineral. Notably, TIMA shows much more potential in distinguishing other homogeneous minerals. For example, it can accurately distinguish between different types of garnets (e.g., grossular, pyrope, almandine, spessartine, and andradite, etc) and amphibole group (e.g., actinolite, katophorite, magnesioanthophyllite, etc) based on differences in chemical element content and color. In this study, TIMA tends to give higher epidote content. This observation may be in part due to the presence of large amounts of altered grains, rock fragments (i.e., particles consisting of more than one mineral) and inclusions in natural samples, which could not be identified by optical methods.

In summary, traditional optical method has the disadvantage of low recognition rates, are time-consuming and relies heavily on operator's experience and subjectivity. The main advantage of TIMA over optical method is that it allows systematic mineralogical mapping of the entire sample field, thus providing a clear and intuitive understanding of the mineral assemblage and sample structure (Xu et al., 2021). The additional information provided by TIMA, such as: backscatter, CL image, phase map and elemental composition (albeit less precise and

semi-quantitative elemental information), is particularly helpful in identifying any one mineral type, making it easier to access specific differences within and between samples (Hrstka et al., 2018; Ward et al., 2018). In particular, TIMA can identify the particle size of a particular mineral in order to facilitate analysis of the size fraction in which a mineral is enriched. However, it remains, unfortunately, impossible to distinguish polycrystalline minerals. Clearly, no technique is immune to bias. Considering the advantages and limitations of these respective techniques, both methods can provide complementary information. Therefore, TIMA should complement rather than replace traditional optical method, and the TIMA results of polymorph mineral need to be verified optically.

## SUMMARY

The heavy mineral composition of the Songhua River drainage sediments provides a best window for assessing the potential impact factors of heavy minerals. In this study, the river and terrace sediments of the Songhua River were taken to construct the heavy mineral composition database based on multi-window (<63  $\mu\text{m}$ , 63–125  $\mu\text{m}$  and 125–250  $\mu\text{m}$ ) and wide-window (63–250  $\mu\text{m}$ ) strategies, and to evaluate the influence of provenance, fluvial processes and chemical weathering on heavy mineral composition. Additionally, the comparison of TIMA SEM-EDS analysis with optical method was discussed. The main conclusions are as follows.

- 1) The tributaries from different parent-rock mountains have distinctly different heavy mineral composition, e.g., the significant enrichment of ilmenite in the Gan River, the Duobukuer River and the Alun River, hematite + lignite in the Gan River, the Duobukuer River, the Alun River and the Yalu River, pyroxene in the Nuomin River, epidote and leucocene in the Great Hinggan Mountains, sphene in the Lesser Hinggan Mountains, and substantially low content of amphibole in the Great Hinggan Mountains, which indicates the role of provenance in controlling heavy mineral composition.
- 2) The natures of basic parent rocks, well preserved in tributaries of the Nenjiang River, tend to be diluted and/or lost in the Nenjiang River and the Songhua River trunk stream, confirming that long-distance river transport-depositional process has led to the ambiguous parent rock information. The significantly different heavy mineral composition in different reaches of the same river (e.g., the Mudan River and the Balan River) indicates the role of fluvial processes in modulating heavy mineral phases and highlights the significance of the number of samples in the source-to-sink system.
- 3) The heavy mineral composition and provenance indexes are significantly affected by hydrodynamic sorting during fluvial processes. By comparison, the low-density minerals are systematically overestimated in a wide window, suggesting a greater advantage of multi-window policy over wide-window policy.

- 4) Based on comparison between river terrace and modern river sediments, the heavy mineral composition of the weakly weathered Songhua River T2 terrace sediments largely retains modern fluvial sediment characteristics. However, the relative enrichment of stable minerals (e.g., ZTR and anatase, etc.) and the strong dissolution of unstable minerals (e.g., amphibole, pyroxene, etc.) in the highly-weathered Tonghe T3 terrace clearly show that chemical weathering plays a key role in controlling heavy-mineral composition of the river terrace samples. Therefore, it is particularly important to first assess the degree of chemical weathering of terrace sediments when using the heavy mineral composition of river terraces for source-sink routing and paleo-drainage evolution studies.
- 5) The TIMA analysis method can better identify the diversity of minerals (More than 40 mineral phases can usually be identified) but performs poorly in identifying polycrystalline minerals.

The integration of the following aspects is fundamental to tackle some of the open problems in sedimentary geology, including (i) the lithology of specific areas, (ii) more amounts of samples, (iii) a flexible and multiple grain-size windows, (iv) selection of sampling locations, and (v) combination of automated and optical methods. This study provides key clues and basic support for further provenance studies and drainage evolution reconstruction in the Songnen Plain, also with a reference for provenance studies in other regions.

## DATA AVAILABILITY STATEMENT

The original contributions presented in the study are included in the article/**Supplementary Material**, further inquiries can be directed to the corresponding author.

## REFERENCES

- Caracciolo, L., Critelli, S., Cavazza, W., Meinhold, G., von Eynatten, H., and Manetti, P. (2015). The Rhodope Zone as a Primary Sediment Source of the Southern Thrace Basin (NE Greece and NW Turkey): Evidence from Detrital Heavy Minerals and Implications for Central-Eastern Mediterranean Palaeogeography. *Int. J. Earth Sci.* 104 (3), 815–832. doi:10.1007/s00531-014-1111-9
- Caracciolo, L., Andò, S., Vermeesch, P., Garzanti, E., McCabe, R., Barbarano, M., et al. (2019). A Multidisciplinary Approach for the Quantitative Provenance Analysis of Siltstone: Mesozoic Mandawa Basin, Southeastern Tanzania. *Geol. Soc. Lond. Spec. Publ.* 484 (1), 275–293. doi:10.1144/SP484-2018-136
- Caracciolo, L. (2020). Sediment Generation and Sediment Routing Systems from a Quantitative Provenance Analysis Perspective: Review, Application and Future Development. *Earth-Sci. Rev.* 209, 103226. doi:10.1016/j.earscirev.2020.103226
- Chen, Q., Song, W. K., Yang, J. K., Hu, Y., Huang, J., Zhang, T., et al. (2021). Principle of Automated Mineral Quantitative Analysis System and its Application in Petrology and Mineralogy: An Example from TESCAN TIMA. *Mineral. Deposits* 40 (2), 245–368. (in Chinese with English abstract). doi:10.16111/j.0258-7106.2021.02.010
- Chew, D., O'Sullivan, G., Caracciolo, L., Mark, C., and Tyrrel, S. (2020). Sourcing the Sand: Accessory Mineral Fertility, Analytical and Other Biases in Detrital U-Pb Provenance Analysis. *Earth Sci. Rev.* 202. doi:10.1016/j.earscirev.2020.103093
- Dunkl, I., von Eynatten, H., Andò, S., Lünsdorf, K., Morton, A., Alexander, B., et al. (2020). Comparability of Heavy Mineral Data - The First Interlaboratory Round Robin Test. *Earth Sci. Rev.* 211, 103210. doi:10.1016/j.earscirev.2020.103210
- Fu, J. Y., Zhu, Q., Yang, Y. J., Zhang, G. Y., and Li, D. T. (2019). *Geological Map of the People's Republic of China (Northeast) (1:1500000)*. Beijing: Geological Press, 1–147. (in Chinese).
- Galehouse, J. S. (1971). "Point Counting," in *Procedures in Sedimentary Petrology*. Editor R. E. Carver (New York: Wiley), 385–407.
- Garzanti, E., and Andò, S. (2007). "Chapter 20 Heavy Mineral Concentration in Modern Sands: Implications for Provenance Interpretation," in *Heavy Minerals in Use. Developments in Sedimentology*. Editors M. A. Mange and D. T. Wright (Amsterdam: Elsevier Science Publishers), 58, 517–545. doi:10.1016/s0070-4571(07)58020-9
- Garzanti, E., Andò, S., Vezzoli, G., Ali Abdel Megid, A., and El Kammar, A. (2006). Petrology of Nile River Sands (Ethiopia and Sudan): Sediment Budgets and Erosion Patterns. *Earth Planet. Sci. Lett.* 252 (3–4), 327–341. doi:10.1016/j.epsl.2006.10.001
- Garzanti, E., Andò, S., and Vezzoli, G. (2008). Settling Equivalence of Detrital Minerals and Grain-Size Dependence of Sediment Composition. *Earth Planet. Sci. Lett.* 273, 138–151. doi:10.1016/j.epsl.2008.06.020

## AUTHOR CONTRIBUTIONS

All authors named on the manuscript have made a significant contribution to the writing, concept, design, execution, or interpretation of the work represented. PW and YX designed the research and experiments; PW, YX, CK and YC performed research; PW, YX, CK, LS, and ZW performed the experiments; All authors analyzed the data; PW wrote the manuscript with help from the other authors.

## FUNDING

This study was financially supported by the National Natural Science Foundation of China (Grant: 42171006 and 41871013) and the Academic Innovation Project of Harbin Normal University (Grant: HSDBSCX 2021-102).

## ACKNOWLEDGMENTS

We thank Mr. Geoffrey Pearce for detailed language polishing. The analysis for heavy minerals was carried out by Peixuan Zhang, Yanzi Zhang, Peng Li, Gentao Wang, Jia Zhou, Xiaofei Wang and Yundan Zhang at the Chengpu and Chengxin Geological Service Co., Ltd, Langfang, China. Jiixin Wang, Siqi Li and Qihang Li are thanked for their assistance in fieldwork and sample pretreatment.

## SUPPLEMENTARY MATERIAL

The Supplementary Material for this article can be found online at: <https://www.frontiersin.org/articles/10.3389/feart.2022.839745/full#supplementary-material>

- Garzanti, E., Andò, S., and Vezzoli, G. (2009). Grain-Size Dependence of Sediment Composition and Environmental Bias in Provenance Studies. *Earth Planet. Sci. Lett.* 277, 422–432. doi:10.1016/j.epsl.2008.11.007
- Garzanti, E. (2019). Petrographic Classification of Sand and Sandstone. *Earth Sci. Rev.* 192, 545–563. doi:10.1016/j.earscirev.2018.12.014
- Haberlah, D., Williams, M. A. J., Halverson, G., McTainsh, G. H., Hill, S. M., Hrstka, T., et al. (2010). Loess and Floods: High-Resolution Multi-Proxy Data of Last Glacial Maximum (LGM) Slackwater Deposition in the Flinders Ranges, Semi-arid South Australia. *Quat. Sci. Rev.* 29 (19–20), 2673–2693. doi:10.1016/j.quascirev.2010.04.014
- HLCC (Harbin Local Chronicles Committee) (1993). *Harbin Chronicles*. Harbin: Heilongjiang People Press, 173–213.
- Honeyands, T., Manuel, J., Matthews, L., O’Dea, D., Pinson, D., Leedham, J., et al. (2019). Comparison of the Mineralogy of Iron Ore Sinters Using a Range of Techniques. *Minerals* 9, 333. doi:10.3390/min9060333
- Hrstka, T., Gottlieb, P., Skála, R., Breiter, K., and Motl, D. (2018). Automated Mineralogy and Petrology - Applications of TESCAN Integrated Mineral Analyzer (TIMA). *J. Geosci.* 63, 47–63. doi:10.3190/jgeosci.250
- Jackson, L. J., Horton, B. K., and Vallejo, C. (2019). Detrital Zircon U-Pb Geochronology of Modern Andean Rivers in Ecuador: Fingerprinting Tectonic Provinces and Assessing Downstream Propagation of Provenance Signals. *Geosphere* 15 (6), 1943–1957. doi:10.1130/ges02126.1
- Johnsson, M. J., and Basu, A. (1993). *Processes Controlling the Composition of Clastic Sediments*, 284. Boulder, Colorado: Geological Society of America 284, 247–261.
- Komar, P. D., and Wang, C. (1984). Processes of Selective Grain Transport and the Formation of Placers on Beaches. *J. Geol.* 92, 637–655. doi:10.1086/628903
- Krippner, A., Meinhold, G., Morton, A. C., Russell, E., and von Eynatten, H. (2015). Grain-Size Dependence of Garnet Composition Revealed by Provenance Signatures of Modern Stream Sediments from the Western Hohe Tauern (Austria). *Sediment. Geol.* 321, 25–38. doi:10.1016/j.sedgeo.2015.03.002
- Krippner, A., Meinhold, G., Morton, A. C., Schönig, J., and von Eynatten, H. (2016). Heavy Minerals and Garnet Geochemistry of Stream Sediments and Bedrocks from the Almklovdalen Area, Western Gneiss Region, SW Norway: Implications for Provenance Analysis. *Sediment. Geol.* 336, 96–105. doi:10.1016/j.sedgeo.2015.09.009
- Lawrence, R. L., Cox, R., Mapes, R. W., and Coleman, D. S. (2011). Hydrodynamic Fractionation of Zircon age Populations. *Geol. Soc. Am. Bull.* 123 (1–2), 295–305. doi:10.1130/b30151.1
- Liu, J., Zhang, J., Miao, X., Xu, S., and Wang, H. (2020). Mineralogy of the Core YRD-1101 of the Yellow River Delta: Implications for Sediment Origin and Environmental Evolution during the Last ~1.9Myr. *Quat. Int.* 537 (30), 79–87. doi:10.1016/j.quaint.2019.12.025
- Mange, M. A., and Wright, D. T. (2007). *Heavy Minerals in Use. Developments in Sedimentology*, 58. Amsterdam: Elsevier, 1329.
- Middleton, G. V. (2003). *Encyclopedia of Sediments and Sedimentary Rocks (Encyclopedia of Earth Sciences Series)*. Dordrecht: Kluwer Academic Publishers, 928.
- Mohammad, A., Bhanu Murthy, P., Dhanamjaya Rao, E. N., and Prasad, H. (2020). A Study on Textural Characteristics, Heavy Mineral Distribution and Grain-Microtextures of Recent Sediment in the Coastal Area between the Sarada and Gosthani Rivers, East Coast of India. *Int. J. Sediment Res.* 35 (05), 484–503. doi:10.1016/j.ijsrc.2020.03.007
- Morton, A. C., and Hallsworth, C. (1994). Identifying Provenance-Specific Features of Detrital Heavy Mineral Assemblages in Sandstones. *Sediment. Geol.* 90 (3–4), 241–256. doi:10.1016/0037-0738(94)90041-8
- Morton, A. C., and Hallsworth, C. R. (1999). Processes Controlling the Composition of Heavy Mineral Assemblages in Sandstones. *Sediment. Geol.* 124, 3–29. doi:10.1016/s0037-0738(98)00118-3
- Morton, A. C., and Hallsworth, C. (2007). “Chapter 7 Stability of Detrital Heavy Minerals during Burial Diagenesis,” in *Heavy Minerals in Use: Developments in Sedimentology*. Editors M.A. Mange and D.T. Wright, 58, 215–245. doi:10.1016/s0070-4571(07)58007-6
- Morton, A. C., Whitham, A. G., and Fanning, C. M. (2005). Provenance of Late Cretaceous to Paleocene Submarine Fan Sandstones in the Norwegian Sea: Integration of Heavy Mineral, Mineral Chemical and Zircon Age Data. *Sediment. Geol.* 182, 3–28. doi:10.1016/j.sedgeo.2005.08.007
- Morton, A. C. (1985). A New Approach to Provenance Studies: Electron Microprobe Analysis of Detrital Garnets from Middle Jurassic Sandstones of the Northern North Sea. *Sedimentology* 32 (4), 553–566. doi:10.1111/j.1365-3091.1985.tb00470.x
- Nie, J., and Peng, W. (2014). Automated SEM-EDS Heavy Mineral Analysis Reveals No Provenance Shift between Glacial Loess and Interglacial Paleosol on the Chinese Loess Plateau. *Aeolian Res.* 13, 71–75. doi:10.1016/j.aeolia.2014.03.005
- Nie, J., Peng, W., Pfaff, K., Möller, A., Garzanti, E., Andò, S., et al. (2013). Controlling Factors on Heavy Mineral Assemblages in Chinese Loess and Red Clay. *Palaeogeogr. Palaeoclimatol. Palaeoecol.* 381–382, 110–118. doi:10.1016/j.palaeo.2013.04.020
- Rubey, W. W. (1933). The Size-Distribution of Heavy Minerals within a Water-Laid Sandstone. *J. Sediment. Res.* 3, 3–29. doi:10.1306/d4268e37-2b26-11d7-8648000102c1865d
- Song, G. L., Liu, Z., and Yu, G. Y. (1986). “Background Contents of Some Elements and Their Environmental Significance in the Main Rock Types of Songhua River Basin, Heilongjiang Province,” in *Natural Science Journal of Harbin Normal University*, 04, 113–121. (in Chinese)CNKI:SUN:HEBY.0.1986-04-016.
- Loon, A. J. V., and Mange, M. A. (2007). “Chapter 6 ‘In Situ’ Dissolution of Heavy Minerals through Extreme Weathering, and the Application of the Surviving Assemblages and Their Dissolution Characteristics to Correlation of Dutch and German Silver Sands,” in *Heavy Minerals in Use*. Editors M. A. Mange and D. T. Wright (Amsterdam: Elsevier), 189–213. doi:10.1016/s0070-4571(07)58006-4
- Vezzoli, G., Garzanti, E., Limonta, M., Andò, S., and Yang, S. (2016). Erosion Patterns in the Changjiang (Yangtze River) Catchment Revealed by Bulk-Sample Versus Single-Mineral Provenance Budgets. *Geomorphology* 261, 177–192. doi:10.1016/j.geomorph.2016.02.031
- von Eynatten, H., Tolosana-Delgado, R., and Karius, V. (2012). Sediment Generation in Modern Glacial Settings: Grain-Size and Source-Rock Control on Sediment Composition. *Sediment. Geol.* 280, 80–92. doi:10.1016/j.sedgeo.2012.03.008
- von Eynatten, H., Tolosana-Delgado, R., Karius, V., Bachmann, K., and Caracciolo, L. (2016). Sediment Generation in Humid Mediterranean Setting: Grain-Size and Source-Rock Control on Sediment Geochemistry and Mineralogy (Sila Massif, Calabria). *Sediment. Geol.* 336, 68–80. doi:10.1016/j.sedgeo.2015.10.008
- Wang, B., Wang, X., Yi, S., Zhao, L., and Lu, H. (2021). Responses of Fluvial Terrace Formation to Monsoon Climate Changes in the North-Eastern Tibetan Plateau: Evidence from Pollen and Sedimentary Records. *Palaeogeogr. Palaeoclimatol. Palaeoecol.* 564, 110196. doi:10.1016/j.palaeo.2020.110196
- Ward, I., Merigot, K., and McInnes, B. I. A. (2018). Application of Quantitative Mineralogical Analysis in Archaeological Micromorphology: A Case Study from Barrow Is., Western Australia. *J. Archaeol. Method Theory* 25, 45–68. doi:10.1007/s10816-017-9330-6
- Weltje, G. J., and von Eynatten, H. (2004). Quantitative Provenance Analysis of Sediments: Review and Outlook. *Sediment. Geol.* 171, 1–11. doi:10.1016/j.sedgeo.2004.05.007
- Weltje, G. J. (2012). Quantitative Models of Sediment Generation and Provenance: State of the Art and Future Developments. *Sediment. Geol.* 280, 4–20. doi:10.1016/j.sedgeo.2012.03.010
- Wu, P., Xie, Y. Y., Kang, C. G., Chi, Y. P., Wei, Z. Y., Wang, J. X., et al. (2020). The Capture of the Songhua River System in the Late Early Pleistocene: Geochemical and Sedimentological Records. *Acta Geol. Sin.* 94 (10), 3144–3160. (in Chinese with English abstract). doi:10.19762/j.cnki.dizhixuebao.2020037
- Wu, P., Xie, Y., Chi, Y., Kang, C., Sun, L., Wei, Z., et al. (2021). Loess Accumulation in Harbin with Implications for Late Quaternary Aridification in the Songnen Plain, Northeast China. *Palaeogeogr. Palaeoclimatol. Palaeoecol.* 570, 110365. doi:10.1016/j.palaeo.2021.110365
- Xie, Y., Yuan, F., Zhan, T., Kang, C., Chi, Y., and Ma, Y. (2018). Geochemistry of Loess Deposits in Northeastern China: Constraint on Provenance and Implication for Disappearance of the Large Songliao Palaeolake. *J. Geol. Soc.* 175, 146–162. doi:10.1144/jgs2017-032

- Xie, Y., Kang, C., Chi, Y., Wu, P., Wei, Z., Wang, J., et al. (2020). Reversal of the Middle-Upper Songhua River in the Late Early Pleistocene, Northeast China. *Geomorphology* 369, 107373. doi:10.1016/j.geomorph.2020.107373
- Xu, M. M., Wei, X. C., Yang, R., Wang, P., and Cheng, X. G. (2021). Research Progress of Provenance Tracing Method for Heavy Mineral Analysis. *Adv. Earth Sci.* 6, 154–171. (in Chinese with English abstract). doi:10.11867/j.issn.1001-8166.2021.021
- Yang, S. Y., and Li, C. X. (1999). Elemental Composition of Modern Surface Sediments of the Yangtze and Yellow River and Their Tracer Effects. *Prog. Nat. Sci.* 9 (10), 68–75. (in Chinese).
- Zhang, X., Pease, V., Omma, J., and Benedictus, A. (2015). Provenance of Late Carboniferous to Jurassic Sandstones for Southern Taimyr, Arctic Russia: A Comparison of Heavy Mineral Analysis by Optical and QEMSCAN Methods. *Sediment. Geol.* 329, 166–176. doi:10.1016/j.sedgeo.2015.09.008
- Zhang, C., Li, Z., Chen, Q., Dong, S., Yu, X., and Yu, Q. (2020). Provenance of Eolian Sands in the Ulan Buh Desert, Northwestern China, Revealed by Heavy Mineral Assemblages. *Catena* 193, 104624. doi:10.1016/j.catena.2020.104624
- Zheng, D., Yang, Q. Y., and Wu, S. H. (2015). *General Comments of Physical Geography of China*. Beijing: Science Press, 186–195. (in Chinese).

**Conflict of Interest:** The authors declare that the research was conducted in the absence of any commercial or financial relationships that could be construed as a potential conflict of interest.

**Publisher's Note:** All claims expressed in this article are solely those of the authors and do not necessarily represent those of their affiliated organizations, or those of the publisher, the editors and the reviewers. Any product that may be evaluated in this article, or claim that may be made by its manufacturer, is not guaranteed or endorsed by the publisher.

Copyright © 2022 Wu, Xie, Kang, Chi, Sun and Wei. This is an open-access article distributed under the terms of the Creative Commons Attribution License (CC BY). The use, distribution or reproduction in other forums is permitted, provided the original author(s) and the copyright owner(s) are credited and that the original publication in this journal is cited, in accordance with accepted academic practice. No use, distribution or reproduction is permitted which does not comply with these terms.